ResearchGate

See discussions, stats, and author profiles for this publication at: https://www.researchgate.net/publication/12872092

Shindo, H. et al. Identification of the DNA binding surface of H-NS protein from Escherichia coli by heteronuclear NMR spectroscopy. FEBS Lett. 455, 63-69

ARTICLE *in* FEBS LETTERS · AUGUST 1999

Impact Factor: 3.17 · DOI: 10.1016/S0014-5793(99)00862-5 · Source: PubMed

CITATIONS
53

READS
20

7 AUTHORS, INCLUDING:

Hiroyuki Ginba
Roche
7 PUBLICATIONS **149** CITATIONS
SEE PROFILE

Chiharu Ueguchi
Nagoya University
63 PUBLICATIONS **3,434** CITATIONS
SEE PROFILE

Available from: Hiroyuki Ginba
Retrieved on: 26 January 2016

FEBS 22313

FEBS Letters 455 (1999) 63–69

Identification of the DNA binding surface of H-NS protein from *Escherichia coli* by heteronuclear NMR spectroscopy

Heisaburo Shindo[a,]*, Ayumi Ohnuki[a], Hiroyuki Ginba[a], Etsuko Katoh[b], Chiharu Ueguchi[c], Takeshi Mizuno[c], Toshimasa Yamazaki[b]

[a]*School of Pharmacy, Tokyo University of Pharmacy and Life Science, Horinouchi, Hachioji, Tokyo 192-03, Japan*
[b]*Structural Biology Unit, National Institute of Agrobiological Resources, 2-1-2 Kannondai, Tsukuba 305, Japan*
[c]*School of Agriculture, Nagoya University, Chikusa-ku, Nagoya 464, Japan*

Received 8 March 1999; received in revised form 14 June 1999

Abstract The DNA binding domain of H-NS protein was studied with various N-terminal deletion mutant proteins and identified by gel retardation assay and heteronuclear 2D- and 3D-NMR spectroscopies. It was shown from gel retardation assay that DNA binding affinity of the mutant proteins relative to that of native H-NS falls in the range from 1/6 to 1/25 for H-NS$^{60-137}$, H-NS$^{70-137}$ and H-NS$^{80-137}$, whereas it was much weaker for H-NS$^{91-137}$. Thus, the DNA binding domain was defined to be the region from residue A80 to the C-terminus. Sequential nuclear Overhauser effect (NOE) connectivities and those of medium ranges revealed that the region of residues Q60–R93 in mutant protein H-NS$^{60-137}$ forms a long stretch of disordered, flexible chain, and also showed that the structure of the C-terminal region (residues A95–Q137) in mutant H-NS$^{60-137}$ was nearly identical to that of H-NS$^{91-137}$. ^{1}H and ^{15}N chemical shift perturbations induced by complex formation of H-NS$^{60-137}$ with an oligonucleotide duplex 14-mer demonstrated that two loop regions, i.e. residues A80–K96 and T110–A117, play an essential role in DNA binding.

© 1999 Federation of European Biochemical Societies.

Key words: H-NS; Nucleoid-associated protein; Deletion mutant; DNA binding domain; Nuclear magnetic resonance; Gel retardation assay

1. Introduction

H-NS protein has many intriguing properties, such as its role in the formation of nucleoid structure, its effect on supercoiled state of plasmids and also its activity as a global transcription regulator [1–5]. H-NS consisting of 137 amino acids is known to be a DNA binding protein that exists as a dimer and binds relatively non-specifically to double stranded DNA [6], but exhibits a certain preference for curved DNA and highly AT-rich DNA fragments [7–11]. Williams et al. [12] showed from analysis of dominant negative mutants of H-NS that the N-terminal domain has a critical role in oligomerization. Site-directed mutagenic studies by Spurio et al. [13] also showed that H-NS proteins with mutations in the regions of residues 112–115 fail to specifically interact with a curved DNA and to repress transcription. Extensive genetic and mutation studies on H-NS by Ueguchi et al. [14,15] identified three distinct functional domains responsible for transcriptional repression (the N-terminal one-third), protein-protein interaction (relatively central portions from residues 21 to 63) and DNA binding domains (the C-terminal half). However, the range of the DNA binding domains is still elusive, because we have only little knowledge of the residues involved in interaction with DNA by point mutation analysis and DNA binding experiments in vitro.

We have previously determined the three-dimensional structure of the C-terminal fragment H-NS$^{91-137}$ of H-NS in solution which has a binding ability to DNA, albeit with very weak affinity [16]. To identify residues interacting with DNA as well as the DNA binding domain in more detail, we have prepared N-terminal deletion mutant proteins of H-NS, i.e. H-NS$^{60-137}$, H-NS$^{70-137}$ and H-NS$^{80-137}$, and investigated their interactions with DNA by heteronuclear NMR spectroscopy. The two loop regions in H-NS were found to be involved in DNA binding, and are discussed in conjunction with biological and genetic studies reported by other investigators.

2. Materials and methods

2.1. Materials

The gene encoding each mutant form of H-NS was amplified from plasmid pHOP11 encoding the H-NS gene [17] and was cloned onto the IPTG-inducible T-7 promoter of a multi-copy plasmid (pT7-7) [18], by which *Escherichia coli* BL21(DE3)pLysn was transformed. Thus, a large amount of uniformly ^{15}N-labeled or ^{15}N/^{13}C doubly labeled mutant proteins can be expressed in this *E. coli* strain upon IPTG induction in synthetic medium M9 containing $^{15}NH_4Cl$ or glucose-$^{13}C_6$, and purified by phosphocellulose P-11 column (Whatman) followed by heparin Sepharose CL6B column (Pharmacia Biotech) as adopted previously for H-NS [16]. To determine the DNA binding domain of H-NS, we have prepared three N-terminal deletion mutant proteins, H-NS$^{80-137}$, H-NS$^{70-137}$ and H-NS$^{60-137}$. Each purified mutant protein showed a single band on SDS-polyacrylamide gel electrophoresis. The sample concentrations were determined by a BCA Protein Assay Reagent (Pierce) using bovine serum albumin as a standard. For NMR measurements, ^{15}N and/or ^{13}C uniformly labeled H-NS$^{60-137}$ was used. The purified sample solution dialyzed against phosphate buffer (0.1 M NaCl, 10 mM phosphate, pH 6.8) was heated at 90°C for 3 min to inactivate a trace of proteases present as impurities in the solution. The solution was concentrated to about 1 mM by Centriprep 3 (Amicon) in a NMR buffer containing 90% H_2O/10% D_2O, 150 mM NaCl, 10 mM KH_2PO_4, 1.0 mM DDT, 0.02% NaN_3, pH 5.5.

DNA with 127 bp composing of a tandem repeat of d(GCGAAAAAAC)$_{10}$ used for gel retardation assay was isolated from *Eco*RI-*Hin*dIII restriction fragments of plasmid pMS101 [19].

The self-complementary oligonucleotide 14-mer, d(CAAAATATATTTTG)$_2$, was purchased as a HPLC grade from Cluachem Inc., and desalted by gel filtration chromatography. The lyophilized sample was dissolved in the NMR buffer adjusted to pH 5.5. Concentration of the DNA was determined by UV absorbance using a relation of 24 o.d. = 1 mg/ml.

2.2. Methods

Gel retardation assay was carried out as described previously [19].

---

*Corresponding author. Fax: (81) (3) 426-4542.
E-mail: shindo@ps.toyaku.ac.jp

0014-5793/99/$20.00 © 1999 Federation of European Biochemical Societies. All rights reserved.

PII: S0014-5793(99)00862-5

Briefly, the *Eco*RI/*Hin*dIII fragment from plasmid pMS101 was labeled with [α-^{32}P]dATP (Amersham) using Klenow fragment (Takara) and purified using a spin column. About 0.15 pmol of the DNA and varying amounts of H-NS or its mutant proteins were mixed in 30 μl of binding buffer containing 10 mM Tris-HCl, pH 7.5, 80 mM NaCl, 1 mM EDTA, 1 mM 2-mercaptoethanol, incubated on ice for 20 min, and then the binding mixtures were applied on to 8% non-denaturing polyacrylamide gel electrophoresis and autoradiographed.

Two- and three-dimensional NMR spectra were recorded on a Bruker DMX-750 (750 MHz for ^{1}H). The spectra were acquired at 25°C with 128 or 256 increments of 1024 complex data points for 2D NMR experiments, and with 48 (f1) and 40 (f2) increments of 1024 complex data points for 3D CBCA(CO)NH [20] and 3D HNCACB [21]. NOE data were obtained from ^{15}N-edited NOESY-HSQC spectra [22] with a mixing time of 100 ms, collecting 96 (f1) and 32 (f2) increments of 1024 complex data points.

3. Results and discussion

3.1. *DNA binding domain of H-NS*

We have examined the state of oligomerization of the mutants used here by gel permeation chromatography with a Superdex 75 HR 10/30 column (Pharmacia Biotech). The results showed that native H-NS, H-NS$^{60-137}$, H-NS$^{70-137}$and H-NS$^{91-137}$ were a tetramer, dimer, trimer and monomer, respectively, at 100 μg of protein/ml in buffer 0.1 NaCl, 10 mM phosphate (pH 6.8). Moreover, mutant H-NS$^{80-137}$ seemed to be in equilibrium between the monomer and dimer. Thus, the region of residues Q60–A80 contributes to oligomerization of H-NS.

Binding affinities of these mutant proteins to 127 bp DNA with a tandem repeat of d(GCGAAAAAAC)$_{10}$ were measured using a gel retardation assay under the same condition as described previously [16], as shown in Fig. 1. For native H-NS (panel a), the gel band of free DNA was retarded at protein concentrations from 0.2 to 0.8 μM, and the lowest concentration at which the gel band was completely displaced from the position of free DNA was about 0.4 μM. Thus, the binding constant of native H-NS to the DNA fragment was estimated to be approximately $K_{\mathrm{asso}} = 2.5 \times 10^6$ M^{-1}, although it is only considered the 'apparent binding constant' for such a non-specific DNA binding protein as H-NS. For H-NS$^{60-137}$ mutant protein (panel b), the gel band was gradually retarded and smeared with increasing protein concentrations, and the complex seemed to aggregate at the highest concentration studied (80 μM). Such a behavior of electrophoresis suggests that the complex formation of native H-NS is cooperative, whereas the mutant proteins bind to DNA in multi-binding mode or undergo a rapid exchange between the bound and unbound states. The concentration at which the gel band began to be retarded from the position of free DNA was in the range of 2.5–10 μM. Thus, the binding strength of the mutant protein relative to that of native H-NS was estimated to be in the range of 1/6 to 1/25. Very similar behavior can be observed for H-NS$^{70-137}$ and H-NS$^{80-137}$ mutant proteins (panels c and d), and both proteins have only little difference in binding affinity. Since relative affinity was about 1/2000 for H-NS$^{91-137}$ [16], it appears that mutant H-NS$^{80-137}$ retains much higher affinity than H-NS$^{91-137}$, demonstrating that the region of residues A80–R90 is essential for the tight DNA binding and that the portion of residues from A80 to the C-terminus is the DNA binding domain of H-NS. However, all the mutant proteins studied here did not exhibit cooperative binding to DNA (see Fig. 1). Considering the lines of evidence that the C-terminal deletion mutant H-NS$^{1-90}$ abolished DNA binding ability and the dimerization core exists in the portion of residues 21–63 [14], some structural requirement (e.g. high oligomerization) is most probably involved in the cooperative DNA binding.

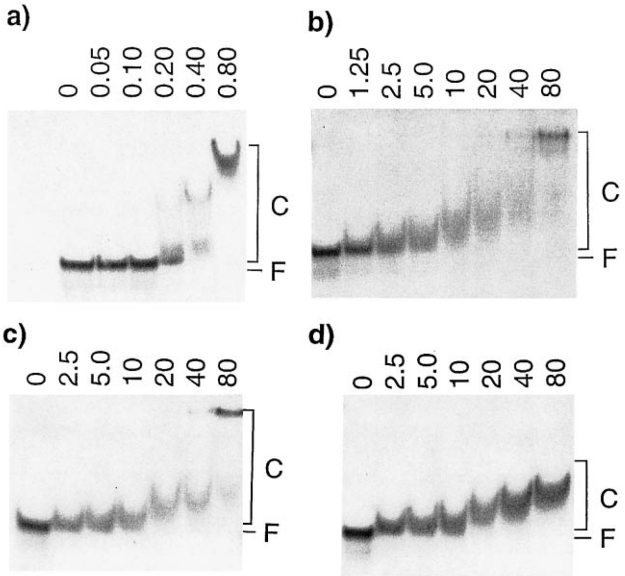

Fig. 1. Autoradiographs of electrophoresis of gel retardation assay for the binding of H-NS and its deletion mutant proteins to a curved DNA. Capital letters F and C represent free DNA and protein-DNA complexes, respectively. Protein concentrations are indicated in μmol/l in each panel: (a) H-NS, (b) H-NS$^{60-137}$, (c) H-NS$^{70-137}$ and (d) H-NS$^{80-137}$.

3.2. *Spectral assignments and the secondary structure of H-NS$^{60-137}$*

As mentioned in Section 2, the solution of mutant H-NS$^{60-137}$ was heated to inactivate a trace of impurities of proteases during NMR measurements. ^{1}H-^{15}N HSQC spectra indicated that the mutant protein was completely reversible to thermal denaturation and that appreciable degradation of the sample did not take place at room temperature for several weeks.

Using a combination of 3D CBCA(CO)NH and 3D HNCACB experiments with ^{15}N/^{13}C doubly labeled H-NS$^{60-137}$, J-coupled sequential connectivities for ^{13}C$^{\alpha}$ and ^{13}C$^{\beta}$ resonances on the ^{15}N-edited, ^{1}H/^{13}C shift correlation spectrum were identified for all residues, with the exception of residues Q60 and G111 which did not show amide signals. All the backbone atoms, amide ^{15}N and ^{1}H, and ^{13}C$^{\alpha}$ including ^{13}C$^{\beta}$ atoms, could be sequentially assigned accordingly. These assignments were in agreement with the proton chemical shifts already reported to H-NS$^{91-137}$ [16]. The obtained chemical shifts were further confirmed by sequential NOE connectivities. NOEs were measured by a ^{15}N-edited NOESY-HSQC experiment with a 100 ms mixing time for uniformly ^{15}N-labeled H-NS$^{60-137}$ mutant protein, and the obtained sequential and medium ranges of NOE connectivities from amide protons are summarized in Fig. 2. The secondary shifts of ^{13}C$^{\alpha}$ and ^{13}C$^{\beta}$ resonances, Δ^{13}C$^{\alpha}$ and Δ^{13}C$^{\beta}$, which are defined as the chemical shift differences of each carbon resonance from that in random coil state, are also shown in Fig. 2.

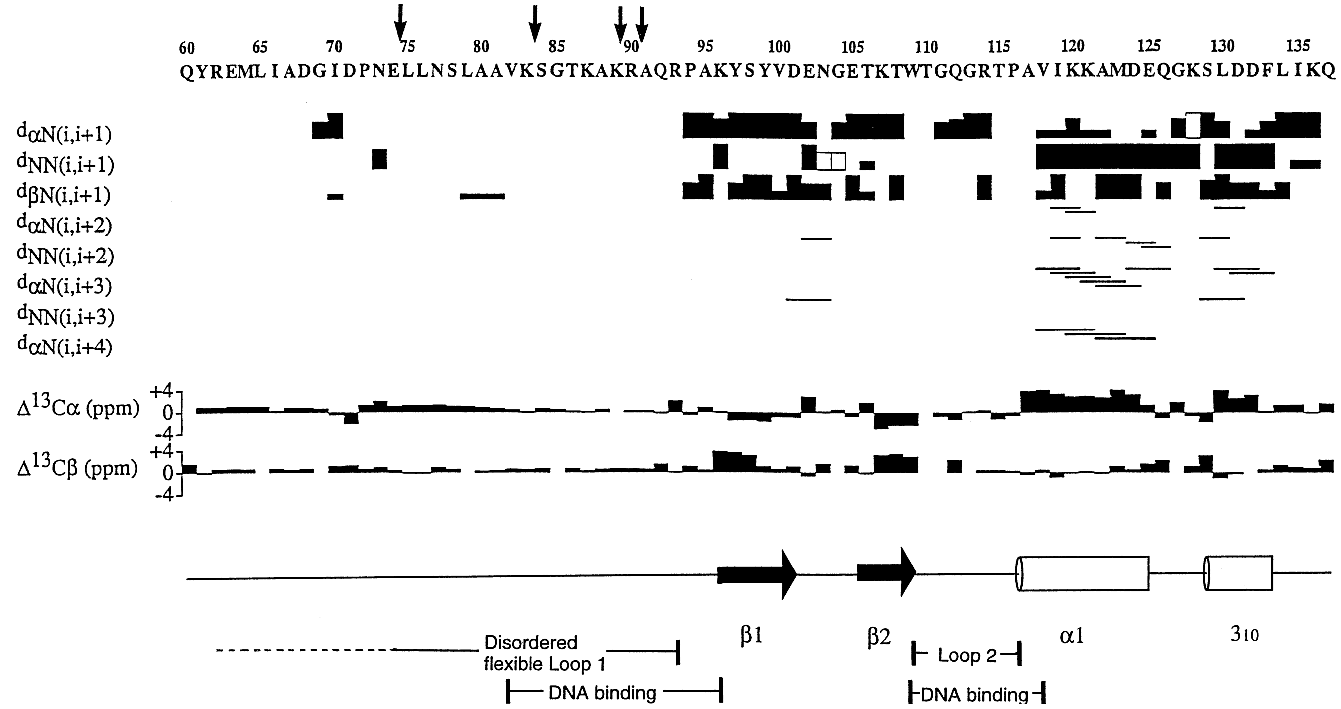

Fig. 2. Sequential and medium ranges of NOE connectivities, secondary shifts of $^{13}C^{\alpha}$ and $^{13}C^{\beta}$ carbon resonances, and structural and functional maps for H-NS$^{60-137}$. Arrows indicated on the amino acid sequence represent cleavage sites of native H-NS by proteases (see details in the text). NOE intensities are indicated by thickness of the bars. Secondary shifts of $\Delta^{13}C^{\alpha}$ and $\Delta^{13}C^{\beta}$ carbon resonances were defined as the difference of the chemical shifts in the native form of protein from that in the random coil state. Secondary structures, β_1, β_2, α and 3_{10} are those as defined in the three-dimensional structure of mutant protein H-NS$^{91-137}$ [16].

Well-defined parts of the secondary structures in the trypsin digestion fragment H-NS$^{91-137}$, as we previously reported [16] were the antiparallel β-strands (Y97–D101 and T106–W109), α-helix (A117–E125) and a short 3_{10}-helix (L130–F133). As can be seen in NOE connectivities for H-NS$^{60-137}$ in Fig. 2, corresponding residues Y97–D101 and T106–T108 in this protein show strong NOEs for $d_{\alpha N(i,i+1)}$ and $d_{\beta N(i,i+1)}$ which are characteristic of the β-sheet form, and residues A117–E125 show strong and medium intensity of NOEs for d_{NN}, weak NOEs for $d_{\alpha N(i,i+3)}$ and $d_{\alpha N(i,i+4)}$ which are typical of the α-helix form. Furthermore, residues L130–F133 show strong NOEs for d_{NN}, weak NOEs for $d_{\alpha N(i,i+3)}$, but no NOE for $d_{\alpha N(i,i+4)}$, consisting with a 3_{10}-helix.

Correlation of $^{13}C^{\alpha}$ and $^{13}C^{\beta}$ chemical shifts with secondary structure have been well documented [23–25]. Relative to random coil chemical shifts, $^{13}C^{\alpha}$ resonances tend to shift upfield in β-strands and extended strand, and they tend to shift downfield in helices. The opposite trend holds for the $^{13}C^{\beta}$ resonances, although this trend is not so sensitive for the helix. As can be seen in Fig. 2, high positive values of secondary shifts $\Delta^{13}C^{\alpha}$ are observed for residues A117–E125 and L130–D132, indicating that these regions are α-helix in nature, whereas high positive values of $\Delta^{13}C^{\beta}$ predict that residues K96–S98 and K107–W109 form a β-sheet. Thus, all the above results of NOEs and secondary chemical shift data are totally in agreement with the view that the secondary structure of the C-terminal domain in H-NS extending from P94 to Q137 (i.e. β-β-loop-α-3_{10} pattern) will be nearly identical between these two truncated mutant proteins, H-NS$^{91-137}$ and H-NS$^{60-137}$.

In contrast to the distinct C-terminal domain, the residues (60–90) in the N-terminal region of H-NS$^{60-137}$ displayed nearly random coil chemical shifts for $^{13}C^{\alpha}$ and $^{13}C^{\beta}$ and no sequential NOE was observed with a few exceptions (residues 68–74 and 79–82), implying that the N-terminal region has no defined secondary structure and therefore it will be a flexible chain in nature. It should be mentioned that major cleavage sites of H-NS by endoproteases were identified by amino acid analysis of major components of digestion fragments. The sites were peptide bonds between two residues, K83/S84, K89/R90 and R90/A91 for trypsin and E74/Leu75 for *Staphylococcus aureus* V8 protease (indicated by arrows at the top of Fig. 2). Thus, the region (residues E74–A90) in intact H-NS is most likely to be a flexible long stretch accessible to proteases.

3.3. Complex formation of H-NS$^{60-137}$ with oligo DNA

H-NS binds non-specifically to double-stranded DNA, but preferentially binds to curved DNA and the AT-rich fragments [6–8]. As a simple starting point, we have deliberately chosen a self-complementary short oligonucleotide, d(CAAAATATATTTTG)$_2$, to identify interaction sites of H-NS on DNA. This DNA 14-mer is A/T-rich and contains two A-tracts. Since titration with DNA into full-length H-NS caused severe line broadening in the ^1H-^{15}N HSQC spectrum, it was difficult to follow individual resonances. Therefore, we have chosen uniformly ^{13}C/^{15}N doubly labeled H-NS$^{60-137}$ protein. A series of ^1H-$^{15}N\{^{13}C\}$ HSQC spectra of the protein were measured as a function of the molar ratio of the self-complementary oligonucleotide to the protein dimer. Fig. 3a shows the ^1H-$^{15}N\{^{13}C\}$HSQC spectra of the H-NS$^{60-137}$ free from DNA, and Fig. 3b compares the expanded portion of the spectra in the absence of the DNA (dark blue) and in the presence of the DNA at 1.4 molar ratio to protein dimer (magenta). All the assignments of the backbone atoms of

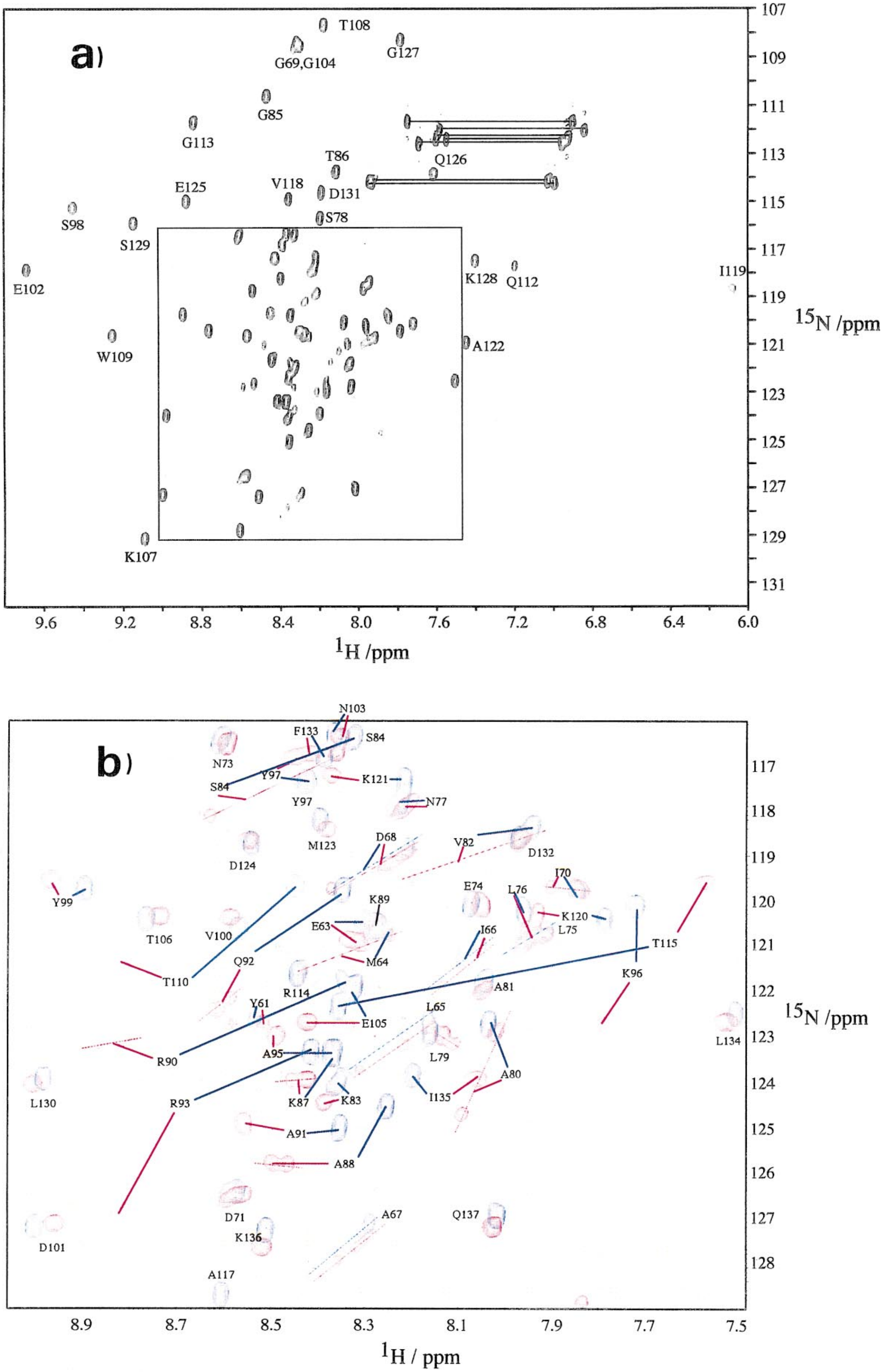
a)
T108
G69,G104
G127
G85
G113
T86
Q126
V118
D131
E125
S78
S98
S129
K128
Q112
I119
E102
W109
A122
K107
107
109
111
113
115
117
119
121
123
125
127
129
131
15N /ppm
9.6
9.2
8.8
8.4
8.0
7.6
7.2
6.8
6.4
6.0
1H /ppm
b)
N103
F133
S84
N73
Y97
K121
S84
Y97
N77
D68
V82
M123
D132
D124
I70
Y99
E74
L76
K89
K120
T106
V100
E63
L75
I66
T115
Q92
M64
T110
K96
R114
A81
Y61
E105
L65
L134
R90
A95
L79
A80
L130
R93
K87
K83
I135
A91
A88
A67
Q137
D71
K136
D101
A117
117
118
119
120
121
122
123
124
125
126
127
128
15N /ppm
8.9
8.7
8.5
8.3
8.1
7.9
7.7
7.5
1H / ppm

Fig. 3. ^{1}H-^{15}N HSQC spectrum of uniformly ^{15}N,^{13}C-labeled H-NS$^{60-137}$ (a), and comparison of the squared region of the spectra (b): free protein (dark blue) and its complex with 14 bp DNA, d(CAAAATATATTTTG)$_2$, at a molar ratio DNA/protein dimer of 1.4 (magenta). The peaks connected by thin lines represent dispersed peaks from the same residues.
←

the protein in the complex with DNA were performed by analyzing 3D HNCACB and CACB(CO)HN of the complex. The assignment of T115 peak which was most perturbed in the complex formation was not straightforward, because two neighboring residues are proline P116 and arginine R114, the latter of which was broaden out on complex formation. However, the observed chemical shifts, 60.25 and 69.95 ppm of $^{13}C^{\alpha}$ and $^{13}C^{\beta}$ of T115 respectively, in the HNCACB spectrum fall into the normal range for threonine and all the threonines other than T115 were readily assigned. Moreover, two correlated peaks (56.35 and 30.76 ppm) of $^{13}C^{\alpha}$ and $^{13}C^{\beta}$ for the preceding residue R114 were identified in the HNCACB spectrum, although its ^{15}N-^{1}H correlation peak was not observed. Thus, the above assignment will be highly reasonable.

It is interesting to note that in the absence of DNA the N-terminal region of residues M64–D68 exhibited dispersed ^{1}H/^{15}N shift correlation peaks as can be seen in the HSQC spectrum (see Fig. 3b), and such dispersed peaks were not affected by the complex formation with DNA. Two possible origins for the dispersed minor peaks are considered: first, the N-terminal portion was partially digested by exoproteases and second, the residues in this portion have a few minor conformations. To examine this, we measured MALDI TOF-MAS spectrum (Voyager-DE RP, PerSeptive Inc.) of non-labeled mutant H-NS$^{60-137}$. Several sequential minor peaks with respective to the main (mass number 8823.6) were observed with exact intervals (±6 mass number) corresponding to the N-terminal sequence, indicating that the mutant protein sustained sequential digestion due to exoprotease activity during purification processes. Thus, the former possibility is more likely as an explanation of the dispersed peaks observed for residues M64–D68.

As is apparent from comparison of the spectra in Fig. 3b, most of the cross peaks were shifted or broadened as titrated with oligonucleotide duplex. Several notable features for DNA binding can be stated as follows. (1) The chemical shift changes were a continuous and monotonous function of the amount of added DNA, and nearly saturated at a 1.4 molar ratio of H-NS dimer to DNA, indicating that the binding is in the fast exchange limit on the NMR time scale. (2) Some peaks such as those of G113, R114 and A117 were completely lost or disappeared in the presence of DNA (Fig. 3b), suggesting that either the free and bound forms or perhaps different forms of protein are in intermediate exchange on the NMR time scale. (3) Some singlet peaks in the absence of DNA split into two peaks in the presence of DNA; those were clustered in a portion of residues from S78 to Q92, especially A80, V82 and S84 exhibited a large separation of the paired peaks. Such a set of paired peaks was reproducible for different sample preparations of protein and DNA, and retained even in the completely saturated state at a high molar ratio of 2.4, indicating that the protein has two different binding modes (discussed later).

Quantifying chemical shift changes in a protein upon ligand binding is a sensitive method for measuring the strength of such interactions and for defining the protein-DNA interaction surface [26–29]. Fig. 4 shows plots of the magnitudes of $^{15}N/^{1}H$ chemical shift changes in the protein induced by DNA binding with respect to residue number. Horizontal bold bars in the upper part of this figure indicate the residues having multiple peak or with the peaks disappeared upon DNA binding. From the chemical shift perturbation pattern, two segments in H-NS$^{60-137}$ are viewed as candidates to directly contribute DNA binding, which are the consecutive residues T110–A117 (or T110–K121) and A80–K96.

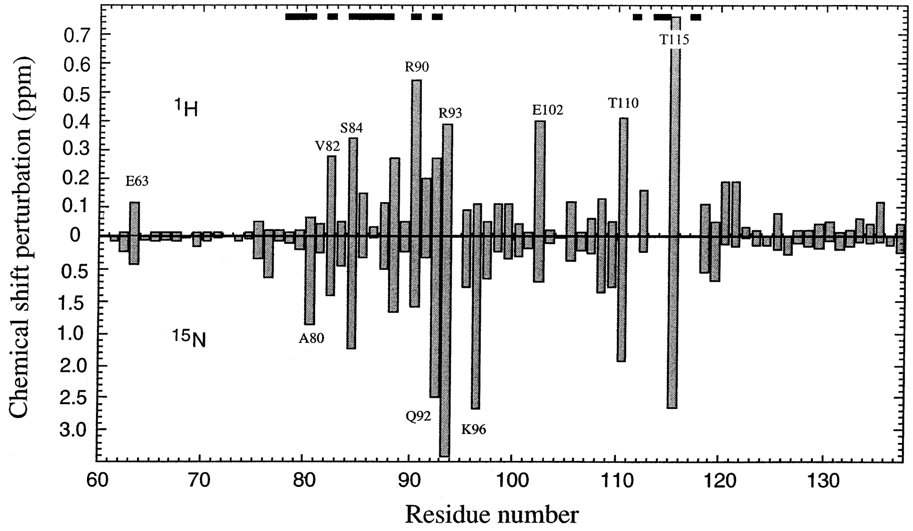

Fig. 4. Histograms of magnitudes of changes in ^{1}H and ^{15}N chemical shifts induced upon complex formation of uniformly $^{15}N/^{13}C$-labeled H-NS$^{60-137}$ with 14 bp DNA versus amino acid residue number. The chemical shifts in the complex were taken as values at a molar ratio of 1.4 DNA/protein dimer as shown in (b). Horizontal bold bars at the top of the figure indicate the residues showing paired peaks and the residues that disappeared in the presence of DNA. In case peaks appear as a pair in the complex, only the chemical shift of the more perturbed peak is presented in the histogram.

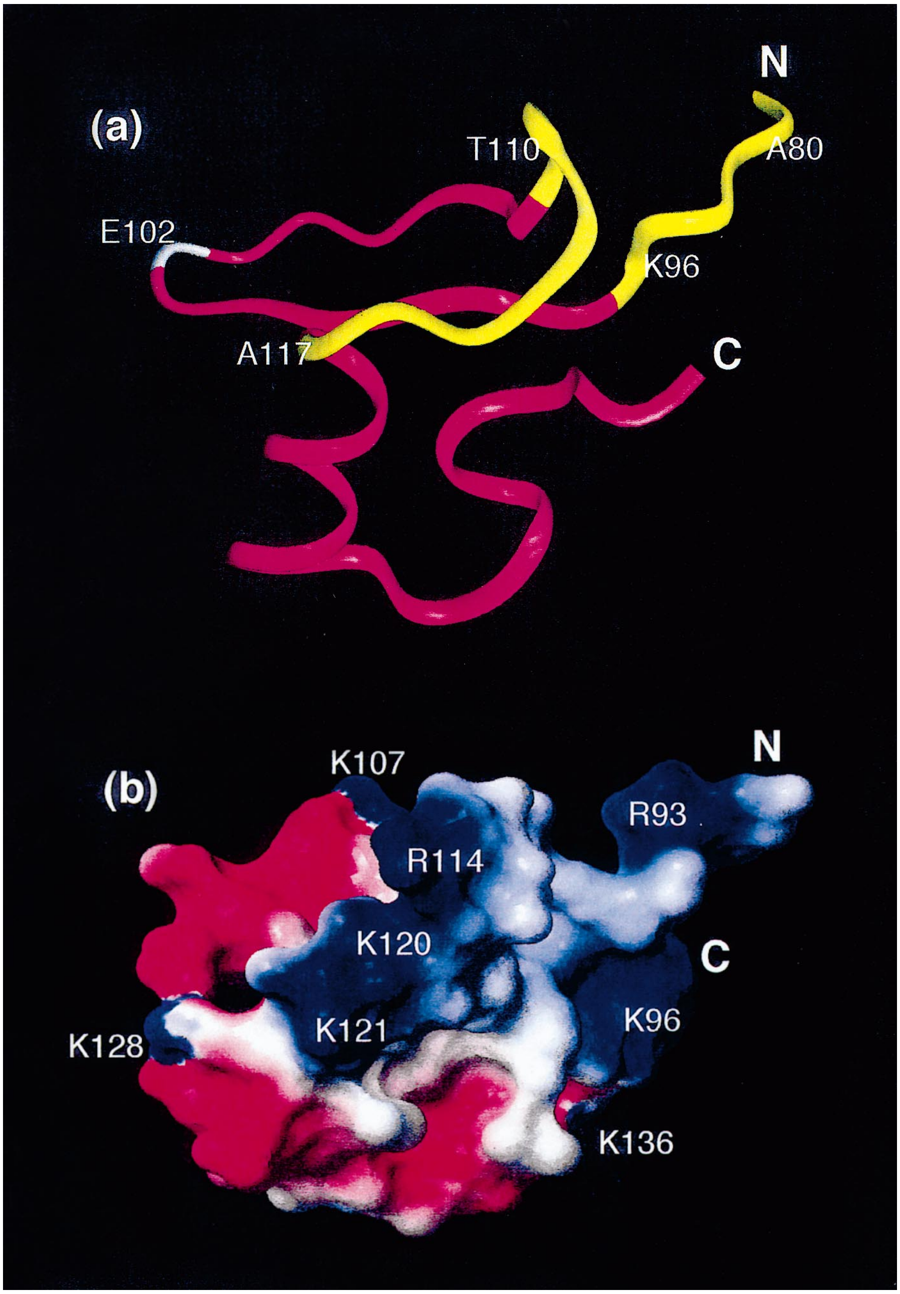

Fig. 5. Ribbon model of the structure of the C-terminal DNA binding domain of H-NS (a), and the electrostatic potential surface of the DNA binding domain (b). The structure was reproduced from Shindo et al. [16].

Regarding the first segment T110–A117, peaks of G113, R114 and A117 were completely broadened out during titration with DNA and the largest shift perturbation ($\Delta\delta = -0.8$ ppm for ^{1}H) was observed for T115. Mutant protein H-NS with a substitution of Gly-113 to Asp had a significant decrease of DNA binding ability [14] and the mutant with single amino acid substitution or deletion of P115 had lost binding preference to a curved DNA as well as the ability of repression in gene transcription [13]. Thus, this region T110–A117 will be directly involved in DNA binding. It should be noted that the region strongly perturbed upon complex formation is identical to loop 2 (T110–P116) in the three-dimensional structure of H-NS$^{91-137}$ (see Figs. 2 and 5).

Within the second segment A80–K96, three basic residues R90, R93 and K96 and one glutamine residue Q92 are strongly perturbed upon DNA binding (Figs. 3b and 4). It is well known that basic residues are commonly used for recognition of the phosphate backbone of DNA and glutamine residue is also frequently used for base recognition by many DNA binding proteins. Thus, in view of the strong chemical shift perturbations for these four resonances and the crucial role of residues 81–90 for DNA binding as suggested by the gel retardation assay, the region of residues A80–K96 is essential for recognition of DNA. This region, which is located at the N-terminal end of antiparallel β-strands, must be a flexible loop, because most of the residues within this region gave no sequential NOE and also they were accessible to proteases in the absence of DNA. Interestingly, as mentioned earlier, many of the residues from A80 to Q92 exhibited pairs of peaks in the complex with 14-mer oligonucleotide, suggesting that each subunit within the H-NS$^{60-137}$ dimer has different binding modes or the dimer asymmetrically binds to the DNA. Although either case cannot ruled out, asymmetric binding is more likely because the paired peaks in the region of A80–Q92 appear with nearly the same intensity in the limit of rapid exchange between the bound and unbound states.

It is interesting to see if a defined secondary structure in the C-terminal loop 1 (L75–P94) is induced upon complex formation. Chemical shift of $^{13}C^{\alpha}$ will be a good monitor for this purpose. $^{13}C^{\alpha}$ atoms of R93 and P94 were shifted downfield by about 0.5–1.1 ppm, respectively, upon complex formation, while most of the other C^{α} carbons in loop 1 were shifted upfield by 0.7 ppm at most (data not shown). The chemical shift perturbations of C^{β} carbons were generally smaller than those of C^{α}. Thus, the magnitude and sense of chemical shift perturbations for both C^{α} and C^{β} carbons rule out any secondary structures in the loop 1 region induced upon complex formation.

In conclusion, we have identified two interacting regions of H-NS with DNA, which consist of residues A80–K96 and T110–A117 located in the C-terminal half of H-NS. Both regions are closely located in space to each other in view of the three-dimensional structure of H-NS$^{91-137}$ (Fig. 5a). Electrostatic potential surface shown in Fig. 5b reveals that these two regions are highly positively charged, which further supports that these two loops form a DNA binding surface on H-NS. Interestingly, none of the secondary structures in H-NS is used for its direct recognition of DNA, unlike the majority of proteins with DNA binding motifs such as helix-turn-helix, bZip, β-ribbon and zinc-finger. In H-NS protein, two disordered flexible loops recognize DNA; flexibility of the recognition sites may explain the non-sequence-specific binding characteristic of H-NS and the oligomeric states of H-NS may be relevant to its preferential binding toward curved DNA.

Acknowledgements: This work was supported by a Grant-in Aid for Science Research from the Ministry of Education, Science, Sports and Culture of Japan (06276104) to H.S.

References

[1] Drilica, K. and Rouviere-Yaniv, J. (1987) Microbiol. Rev. 51, 301–319.
[2] Ueguchi, C. and Mizuno, T. (1993) EMBO J. 12, 1039–1046.
[3] Hayat, M.A. and Mancarella, D.A. (1995) Micron 26, 461–480.
[4] Dorman, C.J. (1995) Microbiology 141, 1271–1280.
[5] Atlung, T. and Ingmer, H. (1997) Mol. Microbiol. 24, 7–17.
[6] Pon, C.L., Calogero, R.A. and Gualerzi, C.O. (1988) Mol. Gen. Genet. 212, 199–202.
[7] Bracco, L., Kotlarz, D., Kolb, A., Dielmann, S. and Buc, H. (1989) EMBO J. 8, 4289–4296.
[8] Yamada, H., Muramatsu, S. and Mizuno, T. (1990) J. Biochem. (Tokyo) 108, 420–425.
[9] Owen-Hughes, T.A., Pavitt, G.D., Santos, D.S., Sidebotham, J.M., Hulton, C.S.J., Hinton, J.C.D. and Higgins, C.F. (1992) Cell 71, 255–265.
[10] Zuber, F., Kotlarz, S., Rimsky, S. and Buc, H. (1994) Mol. Microbiol. 12, 231–240.
[11] Lucht, J.M., Dersch, P., Kempf, B. and Bremer, E. (1994) J. Biol. Chem. 269, 6578–6586.
[12] Williams, R.M., Rimsky, S. and Buc, H. (1996) J. Bacteriol. 178, 4335–4343.
[13] Spurio, R., Falconi, M., Brandi, A., Pon, C.L. and Gualerzi, C.O. (1997) EMBO J. 16, 1795–1805.
[14] Ueguchi, C., Suzuki, T., Yoshida, T., Tanaka, K. and Mizuno, T. (1996) J. Mol. Biol. 263, 149–162.
[15] Ueguchi, C., Seto, C., Suzuki, T. and Mizuno, T. (1997) J. Mol. Biol. 274, 145–151.
[16] Shindo, H., Iwaki, T., Ieda, R., Kurumizaka, H., Ueguchi, C., Mizuno, T., Morikawa, S., Nakamura, H. and Kuboniwa, H. (1995) FEBS Lett. 36, 125–131.
[17] Tanaka, K.-I., Yamada, T., Yoshida, T. and Mizuno, T. (1991) Agric. Biol. Chem. 55, 3139–3141.
[18] Tabor, S. (1989) in: Current Protocols in Molecular Biology (Ausubel, F.M., Brent, R., Kingston, R.E., Moore, D.D., Seidman, J.G., Smith, J.A. and Struhl, K. Eds.), pp. 16.2.1–16.2.11, John Wiley and Son, New York.
[19] Shimizu, M., Miyake, M., Kanke, F., Matsumoto, U. and Shindo, H. (1995) Biochim. Biophys. Acta 1264, 330–336.
[20] Szyperski, T., Pellecchia, M. and Wuethrich, K. (1994) J. Magn. Reson. 105, 188–191.
[21] Grzesiek, S. and Bax, A. (1992) J. Magn. Reson. 99, 201–207.
[22] Fesik, S.W. and Zuiderweg, E.R.P. (1988) J. Magn. Reson. 78, 588–593.
[23] Spera, S. and Bax, A. (1991) J. Am. Chem. Soc. 113, 5490–5492.
[24] Wishart, D.S., Sykes, B.D. and Richards, F.M. (1991) J. Mol. Biol. 222, 311–333.
[25] Fairbrother, W.J., Palmer, A.G., Rance, M., Reizer, J., Saier Jr., M.H. and Wright, P.E. (1992) Biochemistry 31, 4413–4425.
[26] Otting, G., Qian, Y.Q., Billeter, M., Müller, M., Attolter, M., Gehring, W.J. and Wüthrrich, K. (1990) EMBO J. 9, 3085–3092.
[27] Gölach, M., Mittekind, M., Beckman, R.A., Muller, L. and Dreyfuss, G. (1992) EMBO J. 11, 3289–3295.
[28] Chen, Y., Reizer, J., Saier Jr., M.H., Fairbrother, W.J. and Wright, P.E. (1993) Biochemistry 32, 32–37.
[29] Emerson, S.D., Madison, V.S., Palermo, R.E., Waugh, D.S., Scheffler, J.E., Tsao, K.-L., Keifer, S.E., Liu, S.P. and Fry, D.C. (1995) Biochemistry 34, 6911–6918.